

physica **p** status **s** solidi **S**

www.pss-journals.com

reprint



Nano-scale pattern formation on the surface of HgCdTe produced by ion bombardment

A. B. Smirnov*, A. I. Gudymenko, V. P. Kladko, A. A. Korchevyi, R. K. Savkina, F. F. Sizov, and R. S. Udovitska

V. Lashkaryov Institute of Semiconductor Physics, NAS of Ukraine, pr. Nauki 41, C.P. 03028 Kiev, Ukraine

Received 1 October 2014, revised 4 May 2015, accepted 8 July 2015

Published online 27 July 2015

Keywords ion implantation, nanoscale pattern formation, deformation

* Corresponding author: e-mail alex_tenet@isp.kiev.ua, Phone: +38 044 525 5461, Fax: +38 044 525 6296

Presented in this work are the results concerning formation of nano-scale patterns on the surface of a ternary compound $\text{Hg}_{1-x}\text{Cd}_x\text{Te}$ ($x \sim 0.223$). Modification of this ternary chalcogenide semiconductor compound was performed using the method of oblique-incidence ion bombardment with silver ions, which was followed by low-temperature treatment. The energy and dose of implanted

ions were 140 keV and $4.8 \times 10^{13} \text{ cm}^{-2}$, respectively. Atomic force microscopy methods were used for the surface topography characterization. The structural properties of MCT-based structure was analyzed using double and triple crystal X-ray diffraction to monitor the disorder and strain of the implanted region as a function of processing conditions.

© 2015 WILEY-VCH Verlag GmbH & Co. KGaA, Weinheim

1 Introduction A wide spectrum of topological features of a semiconductor surface can be developed by ion bombardment [1]. For example, the implantation of ions of magnetic (or nonmagnetic) metals makes it possible to synthesize nanostructured layers exhibiting both diamagnetic and superparamagnetic, or even ferromagnetic properties in a thin subsurface layer of an irradiated matrix [2]. The formation of composite structures of the “nanocrystalline inclusion-matrix” type is a topical problem of this technology [3].

It is known that low-energy-ion bombardment (tens and hundreds of keV) of semiconductors can lead to a remarkable variety of self-assembled nano-scale patterns whose electronic and optical properties are different from those of bulk materials and might find technological application. The first type of the discovered structures was the periodic height modulations (“ripples”). According to the Bradley-Harper theory [4], ripples are a result of a surface instability caused by the curvature dependence of the sputter yield. It should be noted that now implantation provides a fast and reproducible means of producing a nano-scale pattern on a semiconductor surface subjected both to normal- and to oblique-incidence ion bombardment in a single process step [5–7].

In the previous work [8] it was found that, as a result of the normal-incidence ion implantation with energy ~ 100 keV and subsequent annealing, a remarkable variety of nano-scale patterns depending on the type of the implantable ion (B^+ or Ag^+) is developed on the surface of the *p*- $\text{Hg}_{1-x}\text{Cd}_x\text{Te}/\text{CdZnTe}$ ($x \sim 0.223$). Presented in this work are the results concerning formation of nano-scale pattern on the surface of a ternary chalcogenide semiconductor compound performed using the method of oblique-incidence ion bombardment.

2 Experiment We have carried out a study of mercury cadmium telluride (MCT) thin films subjected to the oblique-incidence (45°) ion bombardment with silver ions, which was followed by low-temperature treatment. The energy and dose of implanted ions were 140 keV and $4.8 \times 10^{13} \text{ cm}^{-2}$, respectively. *P*-type conduction semiconducting $\text{Cd}_x\text{Hg}_{1-x}\text{Te}$ ($x \sim 0.223$) epilayers were grown on [111]-oriented semi-insulating $\text{Cd}_{1-y}\text{Zn}_y\text{Te}$ ($y = 0.04$) substrates from a Te-rich solution at 450°C by liquid-phase epitaxy. The samples were irradiated by Ag^+ ions on the side of the MCT layer on a Vezuvii-5 implanter. Parameters of the MCT region subjected to the ion-induced disordering are presented in Table 1. After the implantation, the

samples were held in the chamber at excess argon pressure 4 bars at a temperature of 75 °C for 5 h. The temperature conditions and the technique of heat treatment of the samples allowed us to avoid the oxidation of the distorted layer and to activate ionic migration in the layer [9].

All processed surfaces were examined using atomic force microscopy with a NanoScope-IIIa Digital Instruments device. The structural characterization of the MCT samples was performed by X-ray diffraction (XRD) using a Panalytical Xpert-pro triple-axis X-ray diffractometer. X-rays were generated from copper linear fine-focus X-ray tube. The $\text{CuK}_{\alpha 1}$ line with a wavelength of 0.15418 nm was selected using a four-bounce (440) Ge monochromator. The experimental schemes allowed two cross-sections of reciprocal lattice sites to be obtained: normally (ω -scanning) and in parallel ($\omega/2\theta$ -scanning) to the diffraction vector. The structural properties of the MCT epilayers were also investigated using X-ray high-resolution reciprocal space mapping (HR-RSM).

Table 1 Parameters of the MCT region subjected to the ion-induced disordering (140 keV Ag^+).

Parameters	45°	0°
Projected range R_p , μm	0.04	0.045
Stragging ΔR_p , μm	0.0186	0.0228
Maximal mechanical stresses σ , Pa	1.284×10^5	1.903×10^5
Maximum doping C_{max} , m^{-3}	3.38×10^{24}	5.25×10^{24}
Vacancy concentration C_v , $\text{N}/\text{\AA}^3$ ion	4.68	4.67
coefficient of crystal lattice contraction β , m^3	1.25×10^{-32}	1.25×10^{-32}

3 Results It was found that the ion irradiation of samples investigated gives rise to the formation of a remarkable variety of nano-scale patterns.

3.1 Surface morphology The AFM image of a surface of a typical MCT sample after implantation is shown in Fig. 1 that demonstrates the formation of an array of nanometer-size objects. AFM characterization has revealed that initial surface demonstrates a grid of quasipores with average diameter ~ 100 nm and the presence of closely packed grains ranging from 40 to 80 nm in dimensions.

The roughness parameter for a $1 \times 1\text{-}\mu\text{m}^2$ surface fragment was around 3.34 nm. The implantation with silver ions at the oblique-incidence geometry gives rise to emergence of a uniform array of nano-islands 5 to 10 nm in height and with a base diameter of 50 to 80 nm (see Fig. 1a). At the same time, AFM image of MCT sample after two normal-incidence ion bombardments with energy 140 keV shows a coarsening of grains to 100 nm in a base diameter and smearing of the initial grain boundaries (see

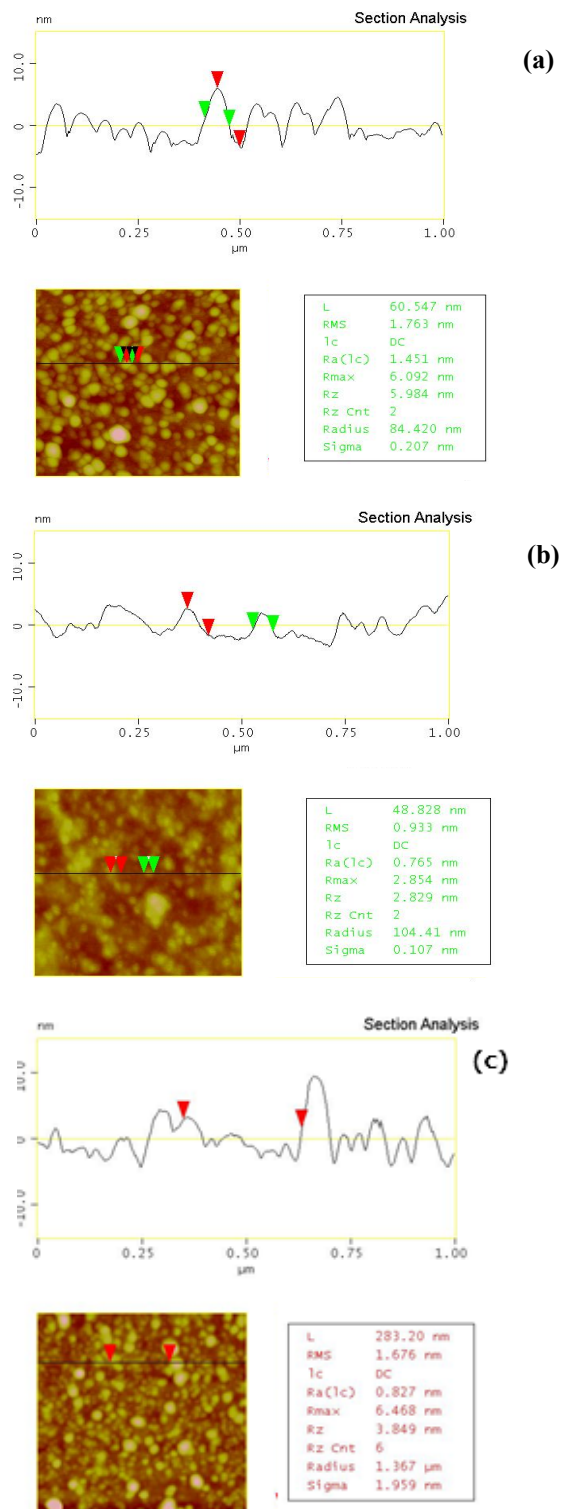


Figure 1 AFM image and surface profile of MCT sample: (a) oblique-incidence ion bombardment with energy 140 keV, $\alpha=45^\circ$; (b) after two normal-incidence ion bombardments with energy 140 keV; (c) virgin surface.

Fig. 1b). It should be noted that the relief became more developed after application of the oblique-incidence geometry (the root-mean-square roughness is about 3.11 nm) in comparison with the normal-incidence geometry where RMS parameter was about 2.17 nm. RMS parameter for the virgin surface was about 1.676 nm.

3.2 X-ray diffraction X-ray rocking curves (RC) for MCT-based structures before and after implantation were obtained from the symmetrical $\omega/2\theta$ -scanning. As seen in Fig. 2, the initial RC has symmetric form whereas the RCs for silver implanted samples have asymmetric form and are characterized by substantial shoulder both on the high and on the low angle sides. XRD results in the coherent-scattering region point out to the tensile strain of the silver implanted MCT layers.

Figures 3(a-c) depict the distribution maps of the diffuse scattering around site 111 in the reciprocal space for the sample of the MCT before and after the silver-ion implantation. The maps are a bonded set of scans perpendicularly (q_x) and parallel (q_z) to the diffraction vector.

The observed distribution of the intensity along axis q_z indicates the existence in the initial material of some structural heterogeneity caused by the existence of the vacancies ($q_z < 0$) and interstitials ($q_z > 0$) (Fig. 3a). And the microdefects system in the initial material is compensated that is confirmed by the symmetric form of the initial RC (see Fig. 2).

After implantation both at the oblique-incidence geometry, and especially at the normal-incidence geometry the significant increase in the half-width of the ω -scan (q_x direction) in the central part of the map is observed (Fig. 3b,c). It can mean the formation of misorientation-type defects as a result of the ion bombardment [10]. Moreover, the appearance of asymmetry in the q_z direction (Fig. 3b, c) points out to the initiation of the tensile deformation in the samples investigated after implantation.

It should be also noted that an additional peak on the low angle sides of RC (Fig. 2, blue curve) as well as peculiarity at $q_z < 0$ on the reciprocal space map of MCT-based heterostructure (Fig. 3c) can mean the formation of the new phase – the polycrystalline MCT with altered composition as it was observed in our previous investigation [8].

Thus, the study of the surface morphology as well as the structural properties of MCT-based structures before and after implantation indicates a nano-scale pattern formation at the application of the oblique-incidence geometry (45°) of the ion bombardment while dual implantation at the normal-incidence geometry results in the significant surface damage.

4 Discussion There are great efforts to interpret the microscopic dynamics of surface roughness and pattern formation induced by ion bombardment. The widely accepted Bradley-Harper theory [4] explains patterns formation by the curvature dependence of the sputtering yield.

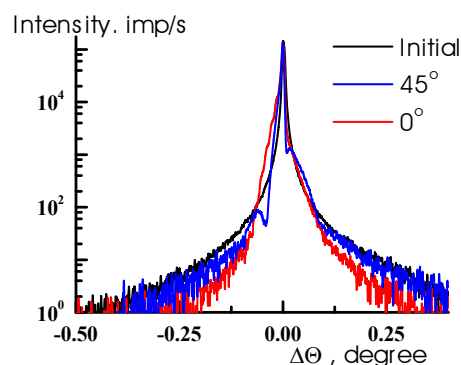


Figure 2 Distribution of the diffuse scattering intensity from the MCT-based heterostructure along the diffraction vector.

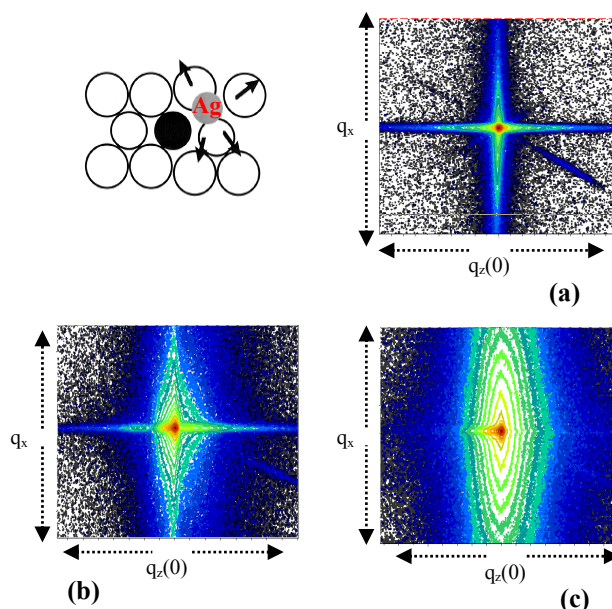


Figure 3 Reciprocal space maps of MCT-based heterostructure obtained from the combined ω and $(\omega-2\theta)$ -scans using high-resolution modules: before implantation (a), after implantation with silver ions at the oblique-incidence geometry (b), after implantation with silver ions at the normal-incidence geometry (c). Inset: ion with a radius comparable to the radius of the matrix atoms penetrates into the crystal lattice.

It was also found the coupling between a surface layer of altered stoichiometry and the topography of the surface obtained as a result of the ion bombardment of the binary compound in particular [11]. An alternative approach is based on the Cueno-Norris theory of the stress relaxation [12]. Obviously, for our experimental conditions a significant erosion is not observed and we cannot apply the full Bradley-Harper model for the explanation of the surface morphology features. According to Sigmund theory [13],

the sputtering yield for MCT is about 11 as well as effective sputtering depth is about 14 Å.

At the same time, knowing that the deformation accumulation is found to lead to the topological instability of the irradiated surface [12] and being based on our investigations we can assume that the deformation fields appearing upon implantation of the studied heterostructure are a significant factor of the observed transformation of its surface. As we know, the deformation sign is dependent on the ratio of ionic radii of the matrix atoms and introduced impurity [14] (see inset Fig. 3). Implantation with ions of small radius (such as B⁺) stimulates the compression of the damaged layer, whereas the implantation with ions of radius comparable with that of Hg (in our case, these are Ag⁺ ions) gives rise to tensile stress in the damaged layer, as confirmed by the X-ray diffraction data obtained in this work and in our previous work [8].

It was found a periodic height modulations or “ripples” induced on the (111) MCT surface by 100 keV B⁺ normal-incidence ion implantation [8]. Whereas the ion implantation by Ag⁺ resulted in a formation of nano-scale mounds on the MCT surface both at the normal incidence, and at the oblique-incidence geometry. In other words, nano-relief induced by ion bombardment is differed for the compressed and stretched surface layers.

Additional factor affecting the surface morphology is the ion migration after implantation. Weak chemical bonds in material under study define the high concentration of electrically active intrinsic defects in accordance with the defect reaction $Hg_i + V_{Hg} = Hg_{Hg}$ [14]. Note that the intrinsic defects, as well as ions, being introduced in MCT, demonstrate high diffusion ability. Taking into account that mercury is driven by the vacancy mechanism, whereas silver, for which $\ln D_0 = f(E_{act})$, $E_{act} = 0.6$ eV is the activation energy [15], moves by the dissociative mechanism, the migration of Hg_i was found to be the dominating process in MCT [16]. The extension regions formed upon silver implantation into MCT shift the reaction to the left, and the compression of deeper layers of the loosened epitaxial film prevent the mercury diffusion into the target depth. Really, in the deformed MCT target, the “healing” of vacancy defects (V_{Hg}) is absent, which is confirmed by preservation of initial porosity in MCT samples after implantation and the following thermal treatment. At the same time, the post-implantation treatment with redundant pressure prohibits Hg_i from moving toward the surface. The compression of deeper layers may be the origin of drawing out silver ions onto the surface. Thus, conditions for appearance and regularities in development of surface relief on surface irradiated with ions, in accord with [12], can be explained by the processes related with ion-induced strains that arise due to saturation of the surface by embedded silver atoms.

The observed effect of nano-structuring can be useful from the viewpoint of developing a new class of electro-optical facility based on MCT that possesses a necessary combination of optical, electro-physical and photoelectric

properties. It was found the presence of some features on the impedance hodograph indicating an appearance of the inductive type impedance.

5 Conclusions Presented in this work are the results concerning of topological features of a semiconductor surface developed by the ion implantation. Modification of Hg_{1-x}Cd_xTe-based structure was performed using the method of oblique-incidence ion bombardment with silver ions (140 keV), which was followed by low-temperature treatment. It was found that a nano-scale pattern formation at the application of the oblique-incidence geometry (45°) of the ion bombardment occurs while dual implantation at the normal-incidence geometry results in the significant damage of the semiconductor surface. The deformation fields appearing upon implantation of the studied heterostructure are a significant factor of the observed transformation of its surface.

References

- [1] J. B. Malherbe, in: *Ion Beam Analysis of Surfaces and Interfaces of Condensed Matter Systems*, edited by P. Chakraborty (Nova Science, New York, 2003), p. 357.
- [2] X. Battle and A. Labarta, *J. Phys. D: Appl. Phys.* **35**, R15 (2002); M. Holdenried and H. Micklitz, *Eur. Phys. J.* **13**, 205 (2000).
- [3] A. Meldrum, R. Lopez, R. H. Magruder, L. A. Boatner, and C. W. White, in: *Materials Science with Ion Beams* (Springer Verlag, Berlin, 2010), pp. 255–285.
- [4] R. M. Bradley and J. M. E. Harper, *J. Vac. Sci. Technol. A* **6**, 2390 (1988).
- [5] S. Facsko, T. Dekorsy, C. Koerdt, C. Trappe, H. Kurz, A. Vogt, and H. L. Hartnagel, *Science* **285**, 1551 (1999).
- [6] Q. M. Wei, X. L. Zhou, B. Joshi, Y. B. Chen, K.-D. Li, Q. M. Wei, K. Sun, and L. M. Wang, *Adv. Mater.* **21**, 2865 (2009).
- [7] F. C. Motta, P. D. Shipman, and R. M. Bradley, *J. Phys. D: Appl. Phys.* **45**, 122001 (2012).
- [8] R. K. Savkina, A. B. Smirnov, A. I. Gudymenko, V. P. Kladko, F. F. Sizov, and C. Frigeri, *Acta Phys. Polon. A* **125**, 1003 (2014).
- [9] Y. Nemirowsky and E. J. Finkman, *Electrochem. Soc.* **126**, 768 (1979).
- [10] A. I. Gusev, *Nanocrystalline Materials: Methods of Preparation and Properties* (Ural Branch of the Russian Academy of Sciences, Yekaterinburg, 1998) [in Russian].
- [11] R. M. Bradley and P. D. Shipman, *Appl. Surf. Sci.* **258**, 4161 (2012).
- [12] L. S. Palatnik, P. G. Cheremskoi, and M. Ya. Fuks, *Pores in Films* (Energoizdat, Moscow, 1982) [in Russian].
- [13] P. Sigmund, *Phys. Rev.* **184**, 183 (1969).
- [14] H. Ebe, M. Tanaka, and Y. Miyamoto, *J. Electron. Mater.* **28**, 854 (1999).
- [15] A. V. Gorshkov, L. A. Bovina, and V. I. Stafeyev, *Fiz. Tekh. Poluprov.* **30**, 1192 (1999) [in Russian].
- [16] F. F. Sizov, R. K. Savkina, A. B. Smirnov, R. S. Udovytyska, V. P. Kladko et al., *Phys. Solid State* **56**, 2160 (2014).